Calculation of Von Kármán's Constant for Turbulent Channel Flow

Steven A. Orszag and Anthony T. Patera
Department of Mathematics, Massachusetts Institute of Technology, Cambridge, Massachusetts 02139
(Received 2 July 1981)

The universal velocity profile for wall-bounded turbulent flows is verified by numerical integration of the incompressible Navier-Stokes equations. Mean velocity profiles, Reynolds stresses, and turbulent intensities are in good agreement with experiment. Von Kármán's constant is calculated to be $\kappa = 0.46 \pm 0.05$.

PACS numbers: 47.25.-c

High-Reynolds-number wall-bounded turbulent flows are extremely sensitive to initial conditions, but their statistical properties are not. Flow past a wall is largely independent of free-stream conditions so that it is a general building block for understanding inhomogeneous, anisotropic turbulence. Although more complicated than homogeneous turbulence, wall flows have been accurately modeled with simple low-order closure methods, but the resulting models do require empirical input.[1] There has not been to date a fundamental demonstration that statistical quantities measured experimentally in wall flows are predictable from the governing equations of fluid dynamics. Here we use a high-resolution numerical simulation of the Navier-Stokes equations to verify the basic scaling features of wall-bounded flows without requiring the resolution of extremely small scales or integration out to very large times. In particular, the computed turbulent mean velocity profile fits the "law of the wall"[2] with von Kármán's constant [see (1) below] $\kappa = 0.46 \pm 0.05$. Here κ governs the dynamics of the inertial layer in which neither geometry nor Reynolds number are important so that universal results may be expected.

Let z be the coordinate normal to the wall and $u_* = (\tau_w/\rho)^{1/2}$ be the friction velocity, where $\tau_w = \nu\, \partial \langle u \rangle / \partial z$ is the mean wall stress, ρ is the fluid density, and ν is the kinematic viscosity. Here $\langle\ \rangle$ denotes an average over the coordinates x, y along the wall, where the mean flow is in the x direction, and the velocity field is $\vec{v} = (u, v, w)$. The wall Reynolds number is $R_* = u_* h/\nu$, where h is the characteristic length. In the channel flow discussed below, h is the channel half-width. In the following, we denote quantities scaled by u_* and h with overbars, while distances measured in terms of the sublayer thickness ν/u_* will be denoted by subscript asterisks.

According to classical scaling arguments,[3] in the outer region (away from the wall) the mean velocity u_{out} does not depend on R_* as $R_* \to \infty$ so that

$$u_{\text{out}} \sim u_* f(\bar{z}) = u_* f(z/h).$$

In the inner region (where z is within order ν/u_* of the wall), the outer scale h is no longer important so that

$$u_{\text{in}} \sim u_* g(z_*) = u_* g(z u_*/\nu).$$

If an intermediate region exists where both the outer and inner scalings hold, then

$$z_* \frac{du_{\text{in}}(z_*)}{dz_*} = \bar{z} \frac{du_{\text{out}}(\bar{z})}{d\bar{z}} = \frac{1}{\kappa}\, u_*.$$

This gives directly a logarithmic velocity region (log layer):

$$\bar{u}_{\text{in}} = \kappa^{-1} \ln z_* + c, \tag{1}$$

where $\bar{u}_{\text{in}} = u_{\text{in}}/u_*$ and κ and c are constants.

The above scalings are independent of R_* as $R_* \to \infty$. This suggests a numerical experiment with R_* sufficiently large that the flow is asymptotic but sufficiently small that all scales can be resolved. However, this spatial scaling analysis only holds for a stationary flow, i.e., as $t \to \infty$. Therefore, before attempting a direct numerical simulation, it is necessary to know the time scale for evolution of the flow.

Here we study the particular case of plane Poiseuille flow, defined as flow between parallel plates driven by a constant pressure gradient of magnitude $2/R$, where R is the Reynolds number based on channel half-width and laminar (parabolic) center-line velocity. No-slip boundary conditions are imposed at the wall and periodicity is assumed in the (x, y) plane with periodicity interval $(2\pi/\alpha, 2\pi/\beta)$. The time-dependent three-dimensional (3D) incompressible Navier-Stokes equations govern the flow in the interior of the channel. We have shown previously[4] that laminar plane Poiseuille flow, $\vec{v} = (1 - z^2)\hat{x}$, is unstable to

© 1981 The American Physical Society

perturbations of the form

$$\vec{v}' = A_{2D}\vec{v}_{2D}(x, z, t) + A_{3D}\vec{v}_{3D}(x, y, z, t). \quad (2)$$

In particular, if A_{2D} is finite while A_{3D} is infinitesimal, one can show that $\vec{v}_{3D}$ grows exponentially in time on a convective time scale. The initial conditions used here are of the form (2) in which $\vec{v}_{2D}(x, y, 0)$ and $\vec{v}_{3D}(x, y, z, 0)$ are eigenmodes of the linear Orr-Sommerfeld problem[5] that depends on (x, y) as $\exp[i(m\alpha x + n\beta y)]$ with $m = \pm 1$, $n = 0$ ($\vec{v}_{2D}$) and $m = \pm 1$, $n = \pm 1$ ($\vec{v}_{3D}$). Near the wall, the perturbation velocities and boundary layer thickness δ scale as $u' = O(v') = O(1)$, while $w' = O(\delta) = O(R^{-1/2})$.[6]

For a stationary flow we clearly require that all statistical quantities equilibrate, and in particular that $dR_*/dt = 0$. However, an integral over all space of the x-momentum equation gives $(\partial/\partial t)\int\langle u\rangle dz = O(1/R)$, where $\langle\ \rangle$ indicates (x, y) averaging. Thus, complete equilibration can only occur on a viscous time scale, and a high-Reynolds-number numerical experiment would appear very costly starting from laminar initial conditions. However, there is also a transition time scale present; on the basis of the scaling of $\vec{v}'$ given above, it is easily shown that $\partial\langle u\rangle/\partial t = O(1/R)$ in the interior and $\partial\langle u\rangle/\partial t = O(1)$ near the wall, where we have also used the fact that the Reynolds stress $-\langle uw\rangle$ is initially uniformly small in the interior. This result implies a fast development of the wall region, which, coupled with the viscous time scales for the interior flow, gives an artificially "blunt" mean profile and correspondingly elevated R_*. Note that such an argument only holds if the perturbation $\vec{v}'$ can sustain itself, i.e., an instability exists. As R_* must eventually return to its initial value,[7] we will obtain $dR_*/dt = 0$, at a finite time, i.e., a quasistationary state where the wall and interior are in balance. At this time universal results should hold. Note also that at this time R_* is a maximum which is optimal for obtaining asymptotic results.

It is also appropriate to comment on the drawbacks of another approach to avoiding long integration times, namely using as initial conditions experimentally obtained statistics.[8] The overall viscous evolution time implies that many flows will change significantly only on a viscous time scale, and hence will appear steady for many convective time scales. Furthermore, such initial conditions do not show that the observed statistics develop naturally from laminar transition structures.

In our work, the Navier-Stokes equations are solved numerically with use of a spectral decomposition of the velocity in terms of Fourier series in x and y and Chebyshev polynomials in z. For the present study we use 64 spectral functions in each of the three directions [i.e., $(64)^3$ modes].[4]

Parameters for the particular run given here are $R = 5000$ and $\alpha = \beta = 1.32$. The initial conditions (2) have two-dimensional energy[9] 0.01 and three-dimensional energy 0.005. The three-dimensional energy is taken finite (as opposed to infinitesimal) to expedite nonlinear interaction. The α and β chosen here give maximum three-dimensional growth.[4] With these parameters the

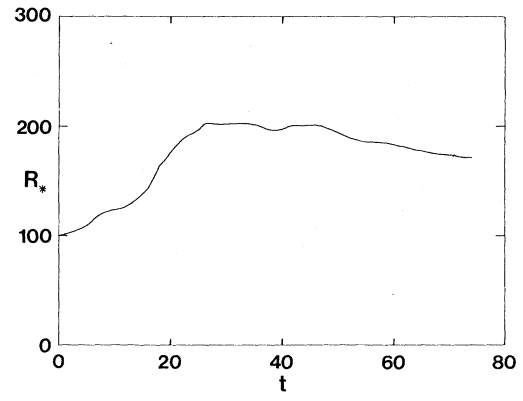

FIG. 1. A plot of the wall Reynolds number $R_* = u_* h/\nu$ as a function of time. R_* initially rises on a convective (transition) time scale and then decays to its initial values on a viscous time scale. When $dR_*/dt = 0$ ($t \simeq 50$) a quasistationary state is achieved.

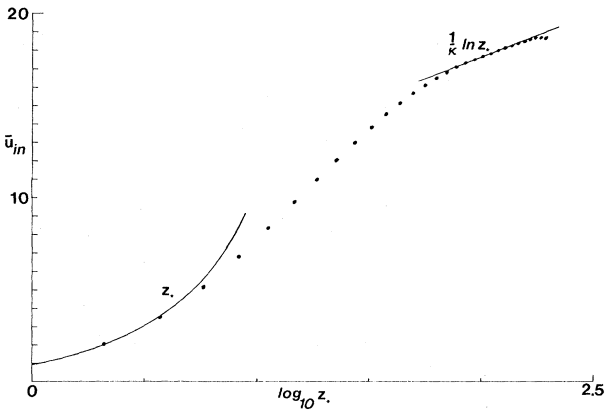

FIG. 2. A plot of the mean velocity u_{in} at $t = 50$ as a function of $\log_{10} z_*$. Note the well developed viscous sublayer (there are three additional grid points that fit $u_{in} \sim u_* z_*$ that lie in the region $\log_{10} z_* < 0$), buffer region, and log layer. The measured von Kármán constant is $\kappa = 0.46 \pm 0.05$.

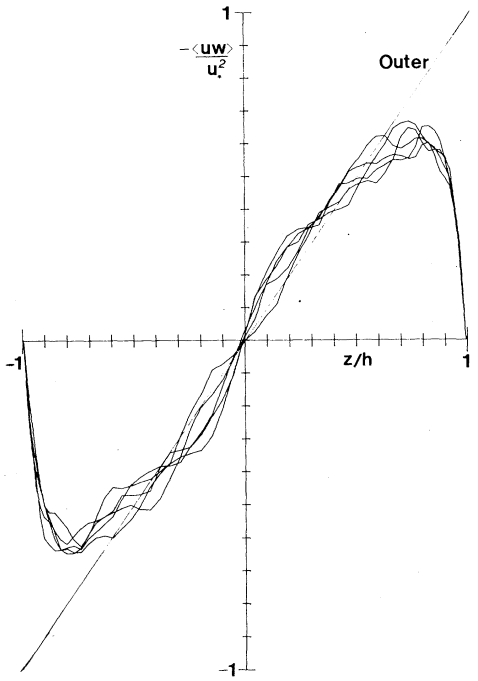

FIG. 3. A plot of the Reynolds stress $-\langle uw\rangle/u_*^2$, as a function of $\bar{z}$ for $t = 50 - 70$ (in steps of 4). Note the good agreement between the numerical solution and the outer ($R \to \infty$) stationary asymptotic solution and the stability of these x-y spatial averages in time.

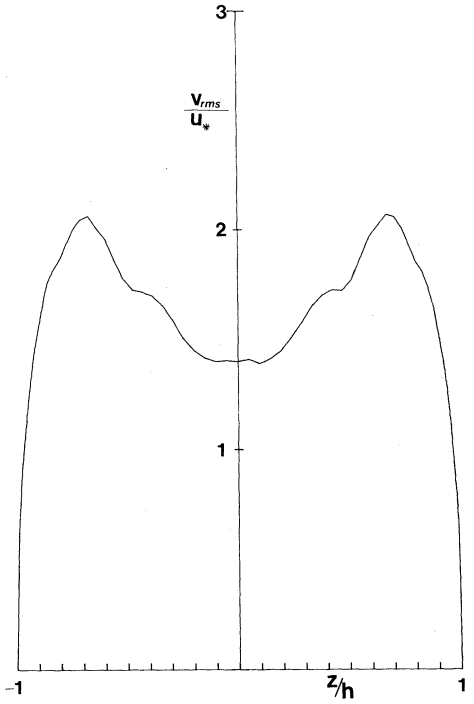

FIG. 4. A plot of the rms spanwise velocity at $t = 50$.

(highly vectorized) code requires less than 10 s per time step on the Cray-1 computer.

A plot of $R_*(t)$ is given in Fig. 1. In accord with the above analysis, R_* rises rapidly to a maximum at $t = t_M \simeq 50$ and then falls off to its initial value on a viscous time scale. At the time t_M, we plot in Fig. 2 $\bar{u}_{in}$ vs $\log_{10} z_*$. Note the good agreement with both experiment[10] and theory: There is a viscous sublayer, $\bar{u}_{in} = z_*$, a "buffer" region, and a log layer (indicated by the straight-line fit) of 8–9 data points giving a von Kármán constant $\kappa = 0.46 \pm 0.05$. At times significantly different from t_M the log layer is not so well developed.

At this point we emphasize that no turbulence modeling has been used[11] and, in particular, all scales of motion from the energy-containing range through the dissipation range are accurately calculated using only the Navier-Stokes equation. To our knowledge, this is the first direct calculation of the von Kármán constant.

In Figs. 3 and 4, we plot the Reynolds stress $-\langle uw\rangle/u_*^2$ and the rms spanwise velocity $\langle v^2\rangle^{1/2}/u_*$, respectively, at t_M. For the Reynolds stress we have plotted the (spatial) averages of $-uw$ at several times around t_M; the stability of these averages in time indicate that the horizontal sample size is sufficiently large. The smooth character of the statistical quantities plotted in Figs. 2–4 should be distinguished from local instantaneous flow quantities that exhibit large turbulent fluctuations.

In conclusion, we emphasize the limitations of our simulation of turbulent channel flows. Periodic boundary conditions have been used which do not completely reflect the true inflow-outflow boundary conditions. Also the slow evolution of the flow to a statistically steady state has necessitated the analysis of intermediate-time results that only partially reflect stationarity. Indeed, the values of the rms spanwise velocity plotted in Fig. 4 are somewhat larger than found experimentally.[10] Nevertheless, the success in simulating the velocity profiles and Reynolds stress distributions of this prototype wall flow suggests that numerical studies of other turbulent flows of practical interest may be feasible.

This work was supported by the U. S. Office of Naval Research under Contracts No. N00014-77-C-0138 and No. N00014-79-C-0478 and the National Science Foundation under Grant No. ATM-8017284. The computations were performed at the Computing Facility of the National Center for

Atmospheric Research, which is supported by the National Science Foundation.

[1]H. Tennekes and J. L. Lumley, *A First Course in Turbulence* (Massachusetts Institute of Technology Press, Cambridge, Mass., 1972), Chap. 5.

[2]T. von Kármán, Nachr. Ges. Wiss. Goettingen Math. Phys. Kl. 58 (1930).

[3]C. B. Millikan, in *Proceedings of the Fifth International Congress on Applied Mechanics* (Wiley, New York, 1939), p. 386.

[4]S. A. Orszag and L. C. Kells, J. Fluid Mech. 96, 159 (1980). See also S. A. Orszag and A. T. Patera, Phys. Rev. Lett. 45, 989 (1980), and to be published.

[5]S. A. Orszag, J. Fluid Mech. 50, 689 (1971).

[6]The scalings near the wall for $\vec{v}'$ and δ in the nonlinear Navier-Stokes equations are the same as for the linear Orr-Sommerfeld equation as nonlinear terms are not dominant in the viscous sublayer.

[7]This follows from x-momentum balance in a time-asymptotic stationary state when periodic boundary conditions are applied downstream.

[8]P. Moin, W. C. Reynolds, and J. H. Ferziger, Stanford University Report No. TF-12, 1978 (unpublished).

[9]Energy is defined here as $\int \vec{v} \cdot \vec{v}\, dx$ normalized with respect to the corresponding quantity for the unperturbed laminar flow.

[10]G. Comte-Bellot, Doctoral thesis, University of Grenoble, 1963 (unpublished). See also J. Laufer, NACA Report No. 1053, 1951 (unpublished).

[11]J. W. Deardorff, J. Fluid Mech. 41, 453 (1970), uses a subgrid scale closure approximation to calculate turbulent channel flow. See also Ref. 8.

Pattern Selection in Rayleigh-Bénard Convection near Threshold

Eric D. Siggia and Annette Zippelius

Laboratory of Atomic and Solid State Physics, Cornell University, Ithaca, New York 14853

(Received 5 June 1981)

A correct long-wavelength theory for convection near onset with free-slip boundary conditions requires two fields and reversible couplings. The wavelengths for which stable rolls exist are dramatically modified when the generation of vertical vorticity is taken into consideration. For small Prandtl numbers and rigid boundaries, the skewed-varicose instability of Busse and Clever is recovered by a plausible but nonrigorous modification of our free-slip equations.

PACS numbers: 47.25.Qv, 03.40.Gc, 47.10.+g

Among the many examples of symmetry breaking and pattern formation in nonequilibrium systems, Boussinesq convection has probably been subject to the most intense experimental and theoretical scrutiny.[1] Because the bifurcation is a continuous one, only a slow modulation of the basic convective roll pattern is allowed by the fluid equations near onset. The time evolution of a general pattern is naturally developed by means of multiscale perturbation theory in terms of a complex amplitude, A, whose phase describes changes in the position and direction of the rolls and whose magnitude modulates the intensity of the convective motion. The dynamical equation for A concisely resolves the question of which of the highly degenerate manifold of linearized solutions to the Boussinesq equations persist and are locally stable when nonlinear effects are included.[2-4] Prior to the work reported here, this equation, to lowest nontrivial order in the deviation of the Rayleigh number or bifurcation parameter, R, from its critical value, R_c, was thought to be purely relaxation, i.e.,

$$dA/dT = -\delta F/\delta A,$$

where F is a local functional of A.[2] As such, it would also settle the question of global stability for the convection problem near onset, since if a small amount of noise were introduced so as to allow the system to sample the manifold of locally stable states accessible to it, the roll pattern would evolve toward the one state that minimizes the potential F.

It therefore came as a surprise when we found that the relaxational equation for A is seriously in error for free-slip boundary conditions when the Prandtl number, P, is finite. The correct equations contain a convective term, which invalidates any statement that could formally have been made about global stability. Furthermore, the band of locally stable wave numbers near onset changes dramatically and for $P \lesssim 10.0$, it is effectively the mirror image of what was previously considered correct.

© 1981 The American Physical Society